

# DPL: Decoupled Prompt Learning for Vision-Language Models

Chen Xu<sup>\*1</sup>, Yuhan Zhu<sup>\*1†</sup>, Guozhen Zhang<sup>1</sup>, Haocheng Shen<sup>2</sup>, Yixuan Liao<sup>2</sup>, Xiaoxin Chen<sup>2</sup>,  
Gangshan Wu<sup>1</sup>, Limin Wang<sup>1,✉</sup>

<sup>1</sup>State Key Laboratory for Novel Software Technology, Nanjing University  
<sup>2</sup>vivo AI Lab

## Abstract

Prompt learning has emerged as an efficient and effective approach for transferring foundational Vision-Language Models (e.g., CLIP) to downstream tasks. However, current methods tend to overfit to seen categories, thereby limiting their generalization ability for unseen classes. In this paper, we propose a new method, Decoupled Prompt Learning (DPL), which reformulates the attention in prompt learning to alleviate this problem. Specifically, we theoretically investigate the collaborative process between prompts and instances (i.e., image patches/text tokens) by reformulating the original self-attention into four separate sub-processes. Through detailed analysis, we observe that certain sub-processes can be strengthened to bolster robustness and generalizability by some approximation techniques. Furthermore, we introduce language-conditioned textual prompting based on decoupled attention to naturally preserve the generalization of text input. Our approach is flexible for both visual and textual modalities, making it easily extendable to multi-modal prompt learning. By combining the proposed techniques, our approach achieves state-of-the-art performance on three representative benchmarks encompassing 15 image recognition datasets, while maintaining parameter-efficient. Moreover, our DPL does not rely on any auxiliary regularization task or extra training data, further demonstrating its remarkable generalization ability.

## Introduction

Learning from the paired text and image data, Vision-Language Models (VLMs) such as CLIP (Radford et al. 2021) have demonstrated remarkable generalization capabilities and robustness across different domains and downstream tasks. These methods learn to align visual and textual representations in the same feature space using separate visual and textual encoders. Pre-trained on a vast dataset of image-text pairs, CLIP exhibits high-quality zero-shot recognition ability on downstream tasks. During inference, class names are combined with hand-crafted templates (e.g., “a photo of a”) and fed into the textual encoder to produce class-specific embeddings. Classification scores

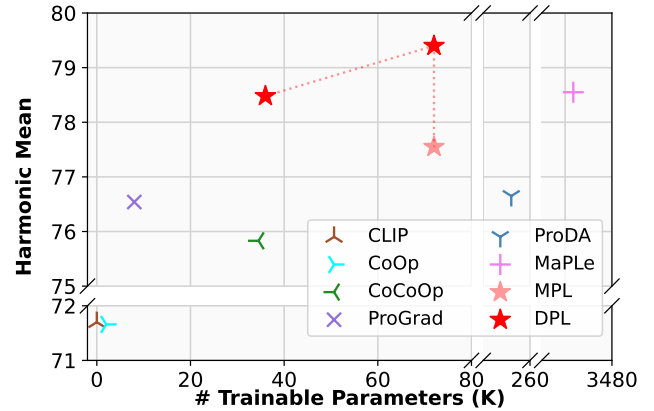


Figure 1: **Comparison with previous prompt learning methods on the average harmonic mean in the base-to-new setting.** DPL surpasses all previous methods by a significant margin while requiring considerably fewer parameters than the previous SOTA. MPL refers to vanilla multi-modal prompt learning.

are then computed as cosine similarities between these textual embeddings and the visual embeddings from visual encoders.

Recently, inspired by the success in NLP, prompt learning has emerged as an effective approach to adapt VLMs to downstream tasks (Zhou et al. 2022b,a; Lu et al. 2022). By replacing hand-crafted templates with learnable embeddings and keeping the model weights frozen, prompt learning enables the model to efficiently learn from downstream tasks and achieve excellent performance in few-shot scenarios (Zhou et al. 2022b). Despite these advantages, such methods often confront the common issue of overfitting to seen classes (Zhou et al. 2022a). As a consequence, performance on unseen classes drops significantly compared to the original pre-trained model. Recent studies have attempted to alleviate this issue by introducing additional auxiliary tasks such as aligning learned prompts closely with hand-crafted templates by using cross-entropy loss (Bulat and Tzimiropoulos 2023) or employing extra learnable modules, e.g., M-Net in CoCoOp (Zhou et al. 2022a) and cross-modal projection layers in MaPLe (Khattak et al. 2023).

<sup>\*</sup>Equal contribution. Listing order is random.

<sup>†</sup>Work is done during internship at vivo AI Lab.

✉: Corresponding author (lmwang@nju.edu.cn).

Unlike previous approaches, in this paper, we focus on decoupling the computation structure in prompt learning and propose a novel method to relieve the overfitting issue. First, we theoretically reformulate and divide the attention process in vanilla prompt learning into four decoupled sub-processes from two perspectives: instance forwarding and prompt forwarding. We then provide detailed explanations for their own function and identify that certain sub-processes can be reinforced to enhance the generalization ability and robustness of the learned prompts. Based on these findings, we propose a novel method called **Decoupled Prompt Learning (DPL)** which recombines the sub-processes in a decoupled manner, resulting in a more generalizable and robust framework for prompts to learn from downstream tasks. We empirically remove the interaction between prompt tokens and provide intuitive speculations and interpretations for this approximation. To further enhance the generalization ability of the text input, we introduce language-conditioned textual prompting, which leverages the prior knowledge from handcrafted templates and preserves the knowledge well with our proposed decoupled attention process. Through comprehensive experiments on three crucial representative settings, including base-to-new generalization, cross-dataset generalization, and domain generalization, DPL surpasses previous state-of-the-art methods on all three benchmarks with fewer parameters (e.g., Fig. 1). Moreover, our DPL does not rely on any additional trainable modules, auxiliary regularization tasks, or extra training data, further demonstrating its superior generalizability and robustness. The main contributions of our work are summarized as follows:

1. We are the first to explore how to improve the computational structure of prompt learning in VLMs. We present an intriguing view on the attention computation of vanilla prompt learning by decomposing it into four sub-processes and identifying the superfluous coupled components which may have an adverse impact on the generalization capability of the pre-trained model.
2. To address these issues, we propose a novel method called Decoupled Prompt Learning (DPL), which effectively decouples the attention process in prompt learning and minimizes unnecessary information interaction that can lead to sub-optimal performance.
3. DPL achieves the state-of-the-art performance on three key representative benchmarks encompassing 15 image recognition datasets, while maintaining parameter-efficient. This verifies the remarkable generalizability of DPL without auxiliary regularization tasks, extra modules, or additional data.

## Related Work

**Vision-Language Models.** Large Vision-Language Models (VLMs) leverage the power of learning joint representations by combine visual and linguistic data during the pre-training stage. These methods have demonstrated remarkable capabilities across a diverse set of challenging tasks. Leading works, such as CLIP (Radford et al. 2021), ALIGN (Jia et al. 2021), Florence (Yuan et al. 2021), LiT (Zhai et al. 2022), DeCLIP (Li et al. 2021), bridge the gap between vision

and language modalities by employing contrastive learning strategies. These techniques enable the model to acquire image and text representations in the same feature space, leveraging the learning on large corpora of text-image pairs (e.g.,  $\sim 400\text{M}$  for CLIP and  $\sim 1\text{B}$  for ALIGN). In this study, we build upon CLIP as the foundation model of our approach and focus on its adaption techniques.

**Prompt Learning.** In Natural Language Processing (NLP) tasks, the introduction of instructive sentences tailored to specific tasks as extra input has been shown to enhance the language model’s ability to generate more contextually relevant outputs (Brown et al. 2020). These sentences, known as text prompts, were initially handcrafted for each individual task. Later works (Lester, Al-Rfou, and Constant 2021; Li and Liang 2021; Liu et al. 2021) replaced handcrafted words with continuous token embeddings and optimized these learnable prompts during training, which is known as “Prompt Learning”. This methodology has demonstrated promising performance in related fields. The technique was extended to the visual modality by Visual Prompt Tuning (Jia et al. 2022), which inserts learnable prompts at each layer of ViT (Jia et al. 2022) to facilitate the adaptation process and confirm its effectiveness.

**Prompt Learning in Vision Language Models.** When applying VLMs (e.g., CLIP (Radford et al. 2021)) to downstream tasks, it is often necessary to design appropriate textual prompts. However, this process can be labor-intensive and sub-optimal. To address this issue, CoOp (Zhou et al. 2022b) proposed to learn text prompts in continuous space and achieve promising results. However, CoCoOp (Zhou et al. 2022a) showed that the learned prompts in the downstream domain are severely overfitted to the seen categories, resulting in poor performance on unseen categories. This undermines the most valuable advantage of CLIP, which is the ability for open-vocabulary classification. To alleviate this problem, follow-up efforts have introduced additional network modules that require more trainable parameters (Zhou et al. 2022a; Lu et al. 2022; Khattak et al. 2023), or auxiliary tasks (Zhu et al. 2022; Yao, Zhang, and Xu 2023; Chen et al. 2022) such as regularizing the learning process using the original CLIP. Other approaches have used additional data (Shen et al. 2022; Ren et al. 2023), or require additional training at test-time (Shu et al. 2022; Zhao et al. 2023). Our proposed DPL investigates the inherent structure of prompt learning and proposes to improve the collaborative process between prompts and instances.

## Method

### Prompt Learning Revisited

Prompt learning was first introduced in (Jia et al. 2022) for computer vision tasks, aiming to efficiently and effectively transfer pre-trained foundational models to downstream tasks. Given a pre-trained Transformer model, learnable prompt tokens are inserted to  $i$ -th layer ( $L_i$ ) while the entire model is kept frozen. We denote the original input instance embeddings and the newly introduced learnable prompts by  $X \in \mathbb{R}^{N \times D}$  and  $P \in \mathbb{R}^{M \times D}$ , respectively. The

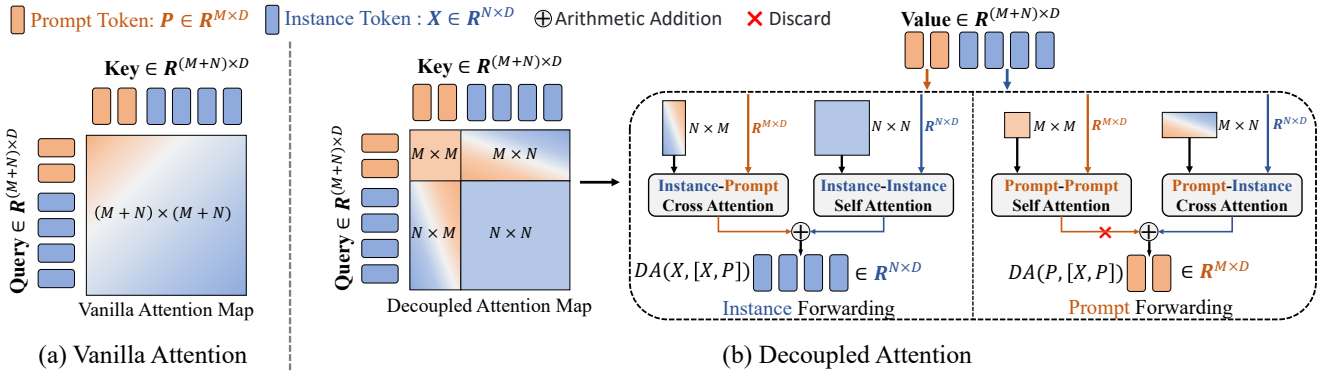


Figure 2: (a) Attention map in vanilla prompt learning. (b) Our decoupled attention for prompt learning. We separate the self-attention within  $[X, P]$  into four decoupled sub-processes, and discard the uninterpretable interaction between prompts.

forward pass of this layer can be formulated as:

$$[O_{i+1}, X_{i+1}] = L_i([P_i, X_i]), \quad (1)$$

where  $[\cdot, \cdot]$  represents the stacking operation along the length of the sequence.  $O_{i+1}$  is the output of corresponding prompt tokens, which can either be discarded (Jia et al. 2022; Khattak et al. 2023), or further utilized by subsequent layers (Zhou et al. 2022b; Xu et al. 2023). For the sake of simplicity, we omit the layer index below.

### Reformulation of Attention in Prompt Learning

For a general attention process, for any query embedding  $y_i \in Y$  as query and  $Z$  as key set, we denote the denominator in the  $\text{softmax}$  function during the calculation of the attention scores as:

$$\lambda_i(Y, Z) = \lambda(y_i, Z) = \sum_{z \in Z} e^{q(y_i)k(z)}, \quad (2)$$

the corresponding attention output of  $y_i$  is denoted by  $\mathcal{A}_i(Y, Z) = \mathcal{A}(y_i, Z) = e^{q(y_i)k(Z)} \times v(Z) / \lambda_i(Y, Z)$ , where  $q, k, v$  are the query, key and value projection functions.

When learnable prompts  $P$  are incorporated, the self-attention process within  $[X, P]$  can be viewed as a self-attention within  $X$ , where the denominator in the  $\text{softmax}$  function is influenced by the introduced prompts and an additional cross-attention to the prompts:

$$\mathcal{A}_i(X, [X, P]) = f_i(X, P)\mathcal{A}_i(X, X) + h_i(X, P)\mathcal{A}_i(X, P), \quad (3)$$

where  $f_i(X, P) + h_i(X, P) = 1$  always holds, and we define  $f_i$  and  $h_i$  as the multiplier of variation of the influenced denominator:

$$\begin{aligned} f_i(X, P) &= \frac{\lambda_i(X, X)}{\lambda_i(X, [X, P])} \\ h_i(X, P) &= \frac{\lambda_i(X, P)}{\lambda_i(X, [X, P])}. \end{aligned} \quad (4)$$

Then we omit the subscript  $i$  to represent the *instance forwarding process* of  $X$  in vanilla prompt learning

$$\mathcal{A}(X, [X, P]) = f(X, P)\mathcal{A}(X, X) + h(X, P)\mathcal{A}(X, P). \quad (5)$$

Similarly, for prompt tokens  $P$ , the *prompt forward process* can be expressed as

$$\mathcal{A}(P, [X, P]) = f(P, X)\mathcal{A}(P, P) + h(P, X)\mathcal{A}(P, X). \quad (6)$$

In Eq. 5 and Eq. 6, the original attention result  $\mathcal{A}([X, P], [X, P])$  in vanilla prompt learning can be separated into four sub-processes that are coupled with each other by their coefficients  $f$  and  $h$ .

### Decoupled Prompt Learning

In this section, we introduce a novel approach called Decoupled Prompt Learning (DPL), aiming at improving the robustness of prompts. Through a detailed analysis of the effectiveness of the four attention sub-processes and we reveal that each of them serves distinct objectives and that certain terms can be reinforced to bolster the robustness and generalization ability without compromising adaption capability. Based on these insights, we introduce DPL, which effectively decouples the overall attention by recombining the decoupled sub-processes to form a more effective and generalizable optimization process in the downstream tasks.

**Instance Forwarding.** We consider two extreme situations from Eq. 5: if  $f_i(X, P) = 1$ , the instance forwarding degrades to zero-shot CLIP, which blocks learning from downstream tasks as  $h_i(X, P) = 0$ . On the other hand, if  $h_i(X, P) = 1$ , the output relies solely on the information extracted from the learned prompts, disregarding the original self-attention result of pre-trained CLIP. Reflecting on these observations, we intuitively assume that the second term is responsible for achieving adaptation goals, whereas the first term, which shares a computational process akin to zero-shot CLIP, could contribute to preserving the generalization ability acquired during the pre-training stage.

Inspired by the above intuition, to emphasize the generalization ability of the model, we focus on analyzing the case where  $f_i(X, P)$  close to 1 for  $\forall x_i \in X$ . Under this assumption, the following limit always holds:

$$\frac{h_i(X, P)}{f_i(X, P)} = \frac{\lambda_i(X, P)}{\lambda_i(X, X)} = \frac{\sum_{p_j \in P} e^{q(x_i)k(p_j)}}{\sum_{x_j \in X} e^{q(x_i)k(x_j)}} \rightarrow 0. \quad (7)$$

This indicates that, after the projections, for a fixed  $N$  and  $M$ , the learned prompts exhibit relatively low similarities with the instance embeddings from the training set. This suggests that such prompts are prevented from forming similar representations to the output distribution of the training subset, allowing them to be less influenced by potential shifts between the testing and training samples in the feature representation space. As a result, they could avoid excessive and over adaptation to downstream datasets and focus more on capturing task-specific information from a global perspective. This characteristic signifies that such learned prompts are more robust and generalizable.

To leverage the aforementioned advantages, we incorporate the assumption that  $f_i(X, P) = 1$  into the instance forwarding process in an approximate manner, while  $h_i(X, P)$  is fairly replaced with an approximate value to the scaled result, denoted as  $\sigma_{X,P} = E[\frac{h_i(X,P)}{f_i(X,P)}] \approx \frac{|P|}{|X|}$ . The prompt length  $|P|$  is typically much smaller than the instance embedding size, ensuring that  $\sigma_{X,P}$  is close to 0. Furthermore, from an optimization perspective, the first term in Eq. 3 could only adjust  $f_i(X, P)$  during the backward process. The learning process for downstream datasets may attempt to reduce  $f_i(X, P)$  to achieve optimization objectives while partially discarding pre-trained knowledge, which brings a potential risk of overfitting. However, this can be avoided in our method since we keep the coefficient constant in our approach.

By formula, the vanilla instance forwarding process is effectively decoupled into two distinct attention processes:

$$\mathcal{DA}(X, [X, P]) = \mathcal{A}(X, X) + \sigma_{X,P}\mathcal{A}(X, P), \quad (8)$$

as shown in the Instance Forwarding part of Fig. 2(b).

**Prompt Forwarding.** It is noteworthy that, despite being non-intuitive in the formula, the original entire self-attention has been decoupled into four *independent* attention subprocesses after decoupling instance forwarding. This necessitates the redefinition of  $f$  and  $h$  in Eq. 6. As in Eq. 8, we approximate the value by the expectations of each coefficient:  $E[f_i(P, X)] \approx \frac{|P|}{|P|+|X|}$  and  $E[h_i(P, X)] \approx \frac{|X|}{|P|+|X|}$ , denoting them as  $\beta_{P,X}$  and  $1 - \beta_{P,X}$ , respectively:

$$\mathcal{DA}_{Re}(P, [X, P]) = \beta_{P,X}\mathcal{A}(P, P) + (1 - \beta_{P,X})\mathcal{A}(P, X). \quad (9)$$

In our practical experiments, we discovered that the first term in Eq. 9 has a detrimental effect on the final generalization performance. Consequently, we remove this term empirically, resulting in the modified equation:

$$\mathcal{DA}(P, [X, P]) = \mathcal{A}(P, X), \quad (10)$$

as illustrated in the Prompt Forwarding part of Fig. 2(b). Upon revisiting the Eq. 9, we recognize that the second term supplements the information about the current input instance, providing subsequent layer prompts with prior knowledge. While the first term appears less interpretable, we surmise that it may introduce extraneous and uninterpretable information for the subsequent layers.

**Language-Conditioned Textual Prompting.** Recent studies (Bulat and Tzimiropoulos 2023; Zhu et al. 2022) suggest

that maintaining the similarity between learned and hand-crafted prompts can lead to more generalizable prompts. Both studies propose auxiliary tasks to achieve this goal, which may introduce additional computational overhead and hyperparameters. Alternatively, a more intuitive approach is to condition textual prompt learning on the hand-crafted sentences by combining learnable prompts with template prompts in the input of the text side. However, vanilla prompt learning significantly disrupts the generalizable knowledge carried by the input templates. In this paper, we introduce the language-condition textual prompting, which builds upon our decoupled prompt learning, where input knowledge can be better preserved. Formally, the input to the text encoder can be expressed as

$$t = [P]_1 [P]_2 \dots [P]_M [\text{Manual Prompt}], \quad (11)$$

where [Manual Prompt] represents the pre-trained CLIP word embeddings of the handcrafted prompts (e.g., “a photo of a [CLS]”).

## Experiments

### Evaluation settings and Datasets

To verify the generalization ability of our method, we evaluate our model in three settings that are widely utilized in prior works (Zhou et al. 2022b,a; Zhu et al. 2022; Lu et al. 2022; Khattak et al. 2023): base-to-new generalization, cross-dataset transfer, and domain generalization.

**Base-to-New Generalization:** For each dataset, we divide the classes equally into two subsets: one serves as the base classes, and the other as the new classes. We train the model on the base classes and evaluate its zero-shot generalization ability on the new classes.

**Cross-Dataset Transfer and Domain Generalization:** In both settings, we train the model on the *source* dataset using a few-shot manner and directly test its zero-shot transfer ability and robustness to visual domain shifts on the *target* datasets.

**Datasets:** As suggested in prior works (Zhou et al. 2022b,a; Khattak et al. 2023), we employ 11 publicly available image classification datasets: ImageNet (Deng et al. 2009) and Caltech101 (Fei-Fei, Fergus, and Perona 2004) for generic object recognition, OxfordPets (Parkhi et al. 2012), StanfordCars (Krause et al. 2013), OxfordFlowers (Nilsback and Zisserman 2008), Food101 (Bossard, Guillaumin, and Gool 2014) and FGVCAircraft (Maji et al. 2013) for fine-grained classification, EuroSAT (Helber et al. 2019) for satellite recognition, UCF101 (Soomro, Zamir, and Shah 2012) for action recognition, DTD (Cimpoi et al. 2014) for texture classification, and finally SUN397 (Xiao et al. 2010) for scene recognition. All 11 datasets are used in the base-to-new setting. We utilize ImageNet as the *source* dataset and the other 10 datasets as *target* datasets for cross-dataset transfer. For domain generalization, we use ImageNet as *source* dataset and select ImageNetV2 (Recht et al. 2019), ImageNet-Sketch (Wang et al. 2019), ImageNet-A (Hendrycks et al. 2021b) and ImageNet-R (Hendrycks et al. 2021a) as *target* datasets.

Methods	Average			ImageNet			Caltech101			OxfordPets		
	Base	New	H	Base	New	H	Base	New	H	Base	New	H
CLIP	69.34	74.22	71.70	72.43	68.14	70.22	96.84	94.00	95.40	91.17	97.26	94.12
CoOp	82.69	63.22	71.66	76.47	67.88	71.92	98.00	89.81	93.73	93.67	95.29	94.47
CoCoOp	80.47	71.69	75.83	75.98	70.43	73.10	97.96	93.81	95.84	95.20	97.69	96.43
ProGrad	81.89	71.85	76.54	76.35	69.26	72.63	97.91	94.40	96.12	94.86	97.52	96.17
ProDA	81.56	72.30	76.65	75.40	70.23	72.72	<b>98.27</b>	93.23	95.68	<b>95.43</b>	97.83	<b>96.62</b>
MaPLe	82.28	75.14	78.55	76.66	70.54	73.47	97.74	94.36	96.02	<b>95.43</b>	97.76	96.58
DPL	<b>83.42</b>	<b>75.76</b>	<b>79.40</b>	<b>77.17</b>	<b>70.92</b>	<b>73.91</b>	98.08	<b>94.54</b>	<b>96.28</b>	95.34	<b>97.89</b>	96.60

---

Methods	StanfordCars			Flowers102			Food101			FGVCAircraft		
	Base	New	H	Base	New	H	Base	New	H	Base	New	H
CLIP	63.37	<b>74.89</b>	68.65	72.08	<b>77.80</b>	74.83	90.10	91.22	90.66	27.19	36.29	31.09
CoOp	<b>78.12</b>	60.40	68.13	97.60	59.67	74.06	88.33	82.26	85.19	<b>40.44</b>	22.30	28.75
CoCoOp	70.49	73.59	72.01	94.87	71.75	81.71	90.70	91.29	90.99	33.41	23.71	27.74
ProGrad	75.17	74.37	74.77	95.44	74.04	83.39	<b>90.73</b>	91.27	91.00	38.88	31.63	34.88
ProDA	74.70	71.20	72.91	<b>97.70</b>	68.68	80.66	90.30	88.57	89.43	36.90	34.13	35.46
MaPLe	72.94	74.00	73.47	95.92	72.46	82.56	90.71	<b>92.05</b>	<b>91.38</b>	37.44	35.61	36.50
DPL	76.16	74.86	<b>75.50</b>	96.39	75.77	<b>84.85</b>	90.46	91.45	90.95	40.40	<b>36.43</b>	<b>38.31</b>

---

Methods	SUN397			DTD			EuroSAT			UCF101		
	Base	New	H	Base	New	H	Base	New	H	Base	New	H
CLIP	69.36	75.35	72.23	53.24	59.90	56.37	56.48	64.05	60.03	70.53	77.50	73.85
CoOp	80.60	65.89	72.51	79.44	41.18	54.24	92.19	54.74	68.69	84.69	56.05	67.46
CoCoOp	79.74	76.86	78.27	77.01	56.00	64.85	87.49	60.04	71.21	82.33	73.45	77.64
ProGrad	80.85	74.93	77.78	77.16	54.63	63.97	88.91	53.75	67.00	84.49	74.52	79.19
ProDA	78.67	76.93	77.79	80.67	56.48	66.44	83.90	66.00	73.88	85.23	71.97	78.04
MaPLe	80.82	78.70	79.75	80.36	59.18	68.16	94.07	<b>73.23</b>	<b>82.35</b>	83.00	78.66	80.77
DPL	<b>81.11</b>	<b>78.84</b>	<b>79.96</b>	<b>81.48</b>	<b>63.53</b>	<b>71.39</b>	<b>95.62</b>	69.31	80.37	<b>85.38</b>	<b>79.79</b>	<b>82.49</b>

Table 1: **Comparison with the state-of-the-art methods on the base-to-new generalization setting.** This result provides persuasive evidence that DPL possesses a remarkable generalization ability while maintaining the superior adaptation ability of prompt learning methods. ‘H’ refers to the harmonic mean of base and new accuracy, highlighting the trade-off between generalization and adaption.

## Implementation Details

Our experiments are conducted on CLIP, based on ViT-B/16, and all results are averaged over three seeds. We employ stochastic gradient descent as the optimizer, following prior works (Zhou et al. 2022b,a; Khattak et al. 2023). All experiments are performed on a single A100 GPU.

Unless otherwise specified, our method is based on *multi-modal prompt learning*, where learnable prompts are incorporated into both the visual and textual sides of CLIP. In the base-to-new setting, we set the visual and textual prompt depth to 9 and set the prompt length per layer to 8 and 4, respectively. All models are trained for 10 epochs with a batch-size of 4. The learning rate is set to 0.1 for visual prompts following (Xu et al. 2023), and 0.002 for textual prompts following (Zhou et al. 2022b,a). For cross-dataset and domain generalization, where ImageNet is used as the training set, we maintain the same setting for the textual side and reduce the visual depth and prompt lengths per layer to 3 and 2, respectively, as both benchmarks rely less on visual priors. The learning rate is set to 0.003 for both visual and textual prompts. We initialize the visual prompts

using Xavier (Glorot and Bengio 2010) following (Jia et al. 2022), and randomly initialize the textual prompts from a normal distribution following (Zhou et al. 2022b; Khattak et al. 2023), except for the first layer, which we initialize from the pre-trained CLIP word embeddings of “a photo of a” following (Khattak et al. 2023). For further experimental details and hyperparameter settings, please refer to the supplementary material.

## Main Results

**Base-to-New Generalization.** In this experimental setup, we present the accuracy of the base and new categories separately, as well as their harmonic mean, which quantifies the trade-off between the two metrics. In Tab. 1, we compare our DPL with previous approaches, including zero-shot CLIP (Radford et al. 2021), CoOp (Zhou et al. 2022b), CoCoOp (Zhou et al. 2022a), ProGrad (Zhu et al. 2022), ProDA (Lu et al. 2022), and MaPLe (Khattak et al. 2023). DPL achieves state-of-the-art performance on both base and new categories, resulting in the highest harmonic mean of 79.40%. Notably, our method only uses 72K trainable pa-

	ImageNet	Caltech101	Pets	Cats	Flowers	Food101	Aircraft	SUN397	DTD	EuroSAT	UCF101	Avg
CLIP	66.73	93.35	88.25	65.48	67.44	83.65	23.67	62.59	44.27	42.01	65.13	63.58
CoOp	<b>71.51</b>	93.70	89.14	64.51	68.71	85.30	18.47	64.15	41.92	46.39	66.55	63.88
CoCoOp	71.02	<b>94.43</b>	90.14	65.32	71.88	86.06	22.94	67.36	45.73	45.37	68.21	65.74
MaPLe	70.72	93.53	90.49	65.57	<b>72.23</b>	86.20	<b>24.74</b>	67.01	<b>46.49</b>	48.06	68.69	66.30
DPL	70.77	93.74	<b>90.67</b>	<b>65.64</b>	71.67	<b>86.36</b>	24.67	<b>67.46</b>	45.76	<b>52.69</b>	<b>70.10</b>	<b>66.88</b>

Table 2: **Comparison of prompt learning methods in cross-dataset transfer setting.** Our method achieves comparable results with state-of-the-art methods on 10 datasets and attains the highest average accuracy, demonstrating its remarkable performance in zero-shot transfer.

	ImageNet	-V2	-S	-A	-R
CLIP	66.73	60.83	46.15	47.77	73.96
CoOp	<b>71.51</b>	<b>64.20</b>	47.99	49.71	75.21
CoCoOp	71.02	64.07	48.75	50.63	76.18
MaPLe	70.72	64.07	49.15	50.90	76.98
DPL	70.77	64.10	<b>49.50</b>	<b>50.92</b>	<b>77.23</b>

Table 3: **Comparison in domain generalization setting.** Our method consistently achieves the highest performance, demonstrating its superior robustness to out-of-distribution scenarios.

rameters, which is  $48\times$  fewer than MaPLe’s 3.39M parameters.

Previous prompt learning methods often suffer from overfitting to seen categories, resulting in poor performance on unseen categories. Prior studies attempt to alleviate such performance drops by introducing extra network modules (Khattak et al. 2023; Zhou et al. 2022a) or auxiliary regularization tasks (Zhu et al. 2022). Both approaches may increase the computation overhead and make the optimization process complicated. In contrast, our method demonstrates superior transfer and generalization performance without introducing any additional trainable parameters or hyperparameters. Specifically, DPL achieves the best performance on 7 out of 11 datasets on new classes and outperforms all previous prompt learning methods on 9 out of 11 datasets, providing strong evidence for the superior generalizability of our proposed decoupled prompt learning.

**Cross-Dataset Transfer.** Tab. 2 presents the results of cross-dataset transfer. DPL achieves comparable performance with previous state-of-the-art methods. Specifically, DPL outperforms all previous methods on 6 out of 10 datasets. Furthermore, our method achieves the best average performance across all datasets, demonstrating the improvement of the zero-shot transfer ability.

**Domain Generalization.** The results of domain generalization are presented in Tab. 3. Our method consistently achieves the best performance on out-of-distribution datasets. These findings demonstrate that our method effectively improves the robustness and generalization of the learned prompts.

## Ablation Studies

**Stepwise Ablation of DPL.** Tab. 4 presents the results of the stepwise ablation analysis of our proposed method. We choose the *vanilla multi-modal prompt learning* (short as MPL) as our baseline, which has the same hyperparameters and training settings as our approach. We gradually decouple the self-attention process within  $[X, P]$  (i.e., combining Eq. 8 and Eq. 9), remove the self-attention within prompt tokens  $P$  (i.e., combining Eq. 8 and Eq. 10), and condition the textual prompt learning on specified template prompts.

We observe a significant improvement of 2.09% in new accuracy achieved by decoupling the attention of the instance and prompt tokens, which highlights the original computational structure of zero-shot CLIP, and ensure that the rich generalizable pre-trained knowledge remains uncompromised when transferring to downstream tasks. Furthermore, removing the self-attention within prompts leads to a further improvement of 0.42%, demonstrating the redundancy of the interactions between prompts. Finally, language-conditioned textual prompting naturally preserves the generalizable ability of the text-side input, resulting in a 0.83% improvement.

Additionally, it is worth noticing that other approaches with similar generalization performance, such as MaPLe, provide much less improvement than we achieve with language-conditioned prompts. This demonstrates the compatibility of LCTP with DPL, where the input knowledge in handcrafted templates is much less disrupted.

**Ablation of Trainable Parameters.** The number of trainable parameters has always been an important metric for the efficiency of prompt learning methods. Tab. 5 compares the number of trainable parameters in DPL with existing prompt learning approaches, while also evaluating the effect of reducing the number of parameters on our method. Our approach is the most parameter-efficient one with  $3.5\times$  fewer parameters than ProDA and  $48\times$  fewer parameters than MaPLe. Moreover, to further understand the relationship between parameters and performance in DPL, we experimented with two manners of halving the number of parameters: (1) halving the number of layers in which prompt tokens are inserted, i.e., from  $1 \rightarrow 9$  to  $1 \rightarrow 4$ ; (2) halving the number of prompt tokens in each layer. Despite the reduction in the number of parameters, our method still exhibits strong generalization to unseen categories, with an av-

Models	DA	SR	LC	Base	New	H
MaPLe				82.28	75.14	78.55
MaPLe			✓	82.26	75.30 (+0.16)	78.63
MPL				83.48	72.42	77.55
	✓			83.21	74.51 (+2.09)	78.62
	✓	✓		83.15	74.93 (+0.42)	78.83
DPL	✓	✓	✓	83.42	75.76 (+0.83)	79.40

Table 4: **Stepwise ablation analysis of our proposed methods**, including Decoupled Attention (DA), Prompt Self-attention Removing (SR), and Language-Conditioned Textual Prompting (LC), demonstrates that our methods consistently and significantly improve the generalization performance while maintaining transferability. Furthermore, we find that LC, when combined with our proposed DA, can better preserve the generalization knowledge, achieving an improvement of 0.83 compared to MaPLe’s 0.16.

Methods	# Params (K)	Base	New	H
CoOp	2	82.69	63.22	71.66
CoCoOp	34.52	80.47	71.69	75.83
ProDA	256	81.56	72.30	76.65
MaPLe	3471.75	82.28	75.14	78.55
DPL	72	<b>83.42</b>	75.76	<b>79.40</b>
DPL <sub>layers/2</sub>	32	81.11	75.19	78.04
DPL <sub>tokens/2</sub>	36	80.81	<b>76.28</b>	78.48

Table 5: **Ablation of trainable parameters.** We experiment with two manners to reduce the number of parameters: halving the number of layers where the prompt is inserted and halving the number of prompts inserted at each layer. Despite the reduction in parameters, our approach maintains excellent generalization performance.

erage accuracy that surpasses all existing approaches.

**DPL is Universally Effective Across Modalities.** We verify the effectiveness of DPL in visual, textual, and visual-textual multimodal settings. To better demonstrate the effects of decoupling attention, we uniformly use language-conditioned textual prompt learning in all experiments except for the single visual modal setting. As shown in Fig. 3, DPL consistently and significantly improves the generalization ability of prompt learning across different modalities by 2.8% in visual, 1.95% in textual, and 2.14% in visual-textual modality. These results highlight the generality of our approach across different modalities.

**Whether DPL Sacrifices Transfer Capability.** In Tab. 4 and Fig. 3, we observe a minor decrease in the base accuracy of our method. This motivates us to investigate whether DPL sacrifices transfer performance compared to vanilla prompt learning. Few-shot learning is an important and representative benchmark to test the model’s adaptation ability. We follow previous works (Zhou et al. 2022b) to train the model on 1, 2, 4, 8, and 16 shots, and evaluate the trained model on the full test sets. The average accuracy across the 11 datasets is shown in Fig. 4. We observe that DPL is slightly

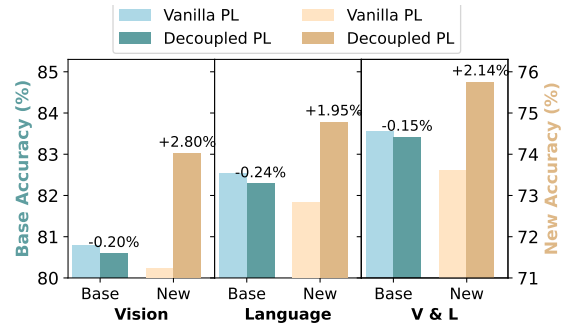


Figure 3: **Ablation of DPL in different modalities.** To better demonstrate the effects of decoupled prompt learning, we uniformly employ LCTP. Our approach significantly enhances generalization when applied to all three settings, demonstrating the universal applicability of our proposed method.

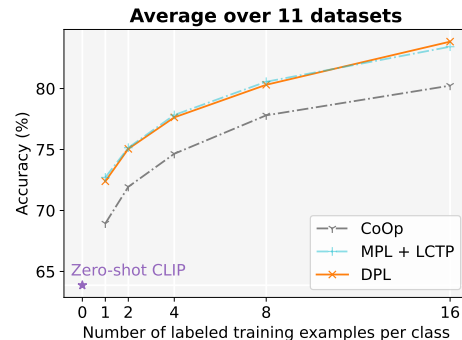


Figure 4: **Few-shot average accuracy over 11 datasets.** This provides convincing evidence that DPL significantly enhances the generalizability of vanilla prompt learning while maintaining its superior adaptation capability.

lower than the baseline (vanilla multi-modal prompt learning with language-conditioned textual prompting, short as MPL+LCTP) for 1, 4, and 8 shots, while marginally outperforming it for 16 shots. Overall, DPL still maintains the excellent transfer ability of prompt learning methods.

## Conclusion

In this paper, we have unveiled the fact that the original attention operation in prompt learning involves four distinct sub-processes. We analyze the potential effectiveness of the separate sub-processes and reveal that each of them is responsible for distinct objectives, and certain terms can be reinforced to bolster the robustness and generalization ability. Based on these insights, we proposed a novel approach called Decoupled Prompt Learning by decoupling the original attention, and achieves a more robust and effective optimization process for prompts by the well-designed recombination of separated sub-processes. Remarkably, our method has achieved the state-of-the-art results on three representative benchmarks without any auxiliary regularization task or additional module. Our improvement in prompt learn-

ing provides a strong and promising baseline for adapting VLMs. We hope it will facilitate research in this field on the generalizability of adapting foundational models.

## References

- Bossard, L.; Guillaumin, M.; and Gool, L. V. 2014. Food-101—mining discriminative components with random forests. In *ECCV*, 446–461.
- Brown, T. B.; Mann, B.; Ryder, N.; Subbiah, M.; Kaplan, J.; Dhariwal, P.; Neelakantan, A.; Shyam, P.; Sastry, G.; Askell, A.; Agarwal, S.; Herbert-Voss, A.; Krueger, G.; Henighan, T.; Child, R.; Ramesh, A.; Ziegler, D. M.; Wu, J.; Winter, C.; Hesse, C.; Chen, M.; Sigler, E.; Litwin, M.; Gray, S.; Chess, B.; Clark, J.; Berner, C.; McCandlish, S.; Radford, A.; Sutskever, I.; and Amodei, D. 2020. Language Models are Few-Shot Learners. In Larochelle, H.; Ranzato, M.; Hadsell, R.; Balcan, M.; and Lin, H., eds., *Advances in Neural Information Processing Systems 33: Annual Conference on Neural Information Processing Systems 2020, NeurIPS 2020, December 6-12, 2020, virtual*.
- Bulat, A.; and Tzimiropoulos, G. 2023. LASP: Text-to-Text Optimization for Language-Aware Soft Prompting of Vision & Language Models. arXiv:2210.01115.
- Chen, G.; Yao, W.; Song, X.; Li, X.; Rao, Y.; and Zhang, K. 2022. Prompt learning with optimal transport for vision-language models. *arXiv preprint arXiv:2210.01253*.
- Cimpoi, M.; Maji, S.; Kokkinos, I.; Mohamed, S.; and Vedaldi, A. 2014. Describing textures in the wild. In *CVPR*, 3606–3613.
- Deng, J.; Dong, W.; Socher, R.; Li, L.-J.; Li, K.; and Fei-Fei, L. 2009. Imagenet: A large-scale hierarchical image database. In *CVPR*, 248–255.
- Fei-Fei, L.; Fergus, R.; and Perona, P. 2004. Learning generative visual models from few training examples: An incremental bayesian approach tested on 101 object categories. In *CVPR-W*, 178–178.
- Glorot, X.; and Bengio, Y. 2010. Understanding the difficulty of training deep feedforward neural networks. In *AISTATS*, 249–256.
- Helber, P.; Bischke, B.; Dengel, A.; and Borth, D. 2019. Eurosat: A novel dataset and deep learning benchmark for land use and land cover classification. *IEEE Journal of Selected Topics in Applied Earth Observations and Remote Sensing*, 12(7): 2217–2226.
- Hendrycks, D.; Basart, S.; Mu, N.; Kadavath, S.; Wang, F.; Dorundo, E.; Desai, R.; Zhu, T.; Parajuli, S.; Guo, M.; et al. 2021a. The many faces of robustness: A critical analysis of out-of-distribution generalization. In *Proceedings of the IEEE/CVF International Conference on Computer Vision*, 8340–8349.
- Hendrycks, D.; Zhao, K.; Basart, S.; Steinhardt, J.; and Song, D. 2021b. Natural adversarial examples. In *Proceedings of the IEEE/CVF Conference on Computer Vision and Pattern Recognition*, 15262–15271.
- Jia, C.; Yang, Y.; Xia, Y.; Chen, Y.-T.; Parekh, Z.; Pham, H.; Le, Q.; Sung, Y.-H.; Li, Z.; and Duerig, T. 2021. Scaling up visual and vision-language representation learning with noisy text supervision. In *ICML*, 4904–4916.
- Jia, M.; Tang, L.; Chen, B.-C.; Cardie, C.; Belongie, S.; Hariharan, B.; and Lim, S.-N. 2022. Visual Prompt Tuning. In *ECCV*. Springer.
- Khattak, M. U.; Rasheed, H.; Maaz, M.; Khan, S.; and Khan, F. S. 2023. Maple: Multi-modal prompt learning. In *Proceedings of the IEEE/CVF Conference on Computer Vision and Pattern Recognition*, 19113–19122.
- Krause, J.; Stark, M.; Deng, J.; and Fei-Fei, L. 2013. 3d object representations for fine-grained categorization. In *ICCV-W*, 554–561. IEEE.
- Lester, B.; Al-Rfou, R.; and Constant, N. 2021. The Power of Scale for Parameter-Efficient Prompt Tuning. In Moens, M.; Huang, X.; Specia, L.; and Yih, S. W., eds., *Proceedings of the 2021 Conference on Empirical Methods in Natural Language Processing, EMNLP 2021, Virtual Event / Punta Cana, Dominican Republic, 7-11 November, 2021*, 3045–3059. Association for Computational Linguistics.
- Li, X. L.; and Liang, P. 2021. Prefix-Tuning: Optimizing Continuous Prompts for Generation. In *ACL*, 4582–4597.
- Li, Y.; Liang, F.; Zhao, L.; Cui, Y.; Ouyang, W.; Shao, J.; Yu, F.; and Yan, J. 2021. Supervision Exists Everywhere: A Data Efficient Contrastive Language-Image Pre-training Paradigm. In *ICLR*.
- Liu, X.; Ji, K.; Fu, Y.; Du, Z.; Yang, Z.; and Tang, J. 2021. P-tuning v2: Prompt tuning can be comparable to fine-tuning universally across scales and tasks. arXiv:2110.07602.
- Lu, Y.; Liu, J.; Zhang, Y.; Liu, Y.; and Tian, X. 2022. Prompt Distribution Learning. In *CVPR*, 5206–5215.
- Maji, S.; Rahtu, E.; Kannala, J.; Blaschko, M.; and Vedaldi, A. 2013. Fine-grained visual classification of aircraft. arXiv:1306.5151.
- Nilsback, M.-E.; and Zisserman, A. 2008. Automated flower classification over a large number of classes. In *ICVGIP*, 722–729.
- Parkhi, O. M.; Vedaldi, A.; Zisserman, A.; and Jawahar, C. 2012. Cats and dogs. In *CVPR*, 3498–3505.
- Radford, A.; Kim, J. W.; Hallacy, C.; Ramesh, A.; Goh, G.; Agarwal, S.; Sastry, G.; Askell, A.; Mishkin, P.; Clark, J.; et al. 2021. Learning transferable visual models from natural language supervision. In *ICML*, 8748–8763. PMLR.
- Recht, B.; Roelofs, R.; Schmidt, L.; and Shankar, V. 2019. Do imagenet classifiers generalize to imagenet? In *International conference on machine learning*, 5389–5400. PMLR.
- Ren, S.; Zhang, A.; Zhu, Y.; Zhang, S.; Zheng, S.; Li, M.; Smola, A.; and Sun, X. 2023. Prompt Pre-Training with Twenty-Thousand Classes for Open-Vocabulary Visual Recognition. *arXiv preprint arXiv:2304.04704*.
- Shen, S.; Yang, S.; Zhang, T.; Zhai, B.; Gonzalez, J. E.; Keutzer, K.; and Darrell, T. 2022. Multitask vision-language prompt tuning. *arXiv preprint arXiv:2211.11720*.
- Shu, M.; Nie, W.; Huang, D.-A.; Yu, Z.; Goldstein, T.; Anandkumar, A.; and Xiao, C. 2022. Test-time prompt tuning for zero-shot generalization in vision-language models.



*Advances in Neural Information Processing Systems*, 35: 14274–14289.

Soomro, K.; Zamir, A. R.; and Shah, M. 2012. UCF101: A dataset of 101 human actions classes from videos in the wild. arXiv:1212.0402.

Wang, H.; Ge, S.; Lipton, Z.; and Xing, E. P. 2019. Learning robust global representations by penalizing local predictive power. *Advances in Neural Information Processing Systems*, 32.

Xiao, J.; Hays, J.; Ehinger, K. A.; Oliva, A.; and Torralba, A. 2010. Sun database: Large-scale scene recognition from abbey to zoo. In *CVPR*, 3485–3492.

Xu, C.; Shen, H.; Shi, F.; Chen, B.; Liao, Y.; Chen, X.; and Wang, L. 2023. Progressive Visual Prompt Learning with Contrastive Feature Re-formation. arXiv:2304.08386.

Yao, H.; Zhang, R.; and Xu, C. 2023. Visual-language prompt tuning with knowledge-guided context optimization. In *Proceedings of the IEEE/CVF Conference on Computer Vision and Pattern Recognition*, 6757–6767.

Yuan, L.; Chen, D.; Chen, Y.-L.; Codella, N.; Dai, X.; Gao, J.; Hu, H.; Huang, X.; Li, B.; Li, C.; et al. 2021. Florence: A new foundation model for computer vision. arXiv:2111.11432.

Zhai, X.; Wang, X.; Mustafa, B.; Steiner, A.; Keysers, D.; Kolesnikov, A.; and Beyer, L. 2022. Lit: Zero-shot transfer with locked-image text tuning. In *CVPR*, 18123–18133.

Zhao, S.; Wang, X.; Zhu, L.; and Yang, Y. 2023. Test-Time Adaptation with CLIP Reward for Zero-Shot Generalization in Vision-Language Models. *arXiv preprint arXiv:2305.18010*.

Zhou, K.; Yang, J.; Loy, C. C.; and Liu, Z. 2022a. Conditional prompt learning for vision-language models. In *CVPR*, 16816–16825.

Zhou, K.; Yang, J.; Loy, C. C.; and Liu, Z. 2022b. Learning to prompt for vision-language models. *International Journal of Computer Vision*, 130(9): 2337–2348.

Zhu, B.; Niu, Y.; Han, Y.; Wu, Y.; and Zhang, H. 2022. Prompt-aligned Gradient for Prompt Tuning. arXiv:2205.14865.

## Supplementary Material

### Detailed Derivation of the Attention Reformulation

Here we present a comprehensive formula derivation for the separate results of the attention process within the vanilla prompt learning. Utilizing the definitions provided in the main paper and accounting for the constant term as  $\sqrt{D}$ , we obtain the following equation:

$$\mathcal{A}([X, P], [X, P]) = [\mathcal{A}(X, [X, P]), \mathcal{A}(P, [X, P])], \quad (12)$$

as the original instance and prompt forwarding processes respectively. And for a token embedding  $x_i \in X$ , we have:

$$\begin{aligned} \mathcal{A}_i(X, [X, P]) &= \frac{\sum_{y_j \in [X, P]} e^{q(x_i)k(y_j)} v(y_j)}{\lambda_i(X, [X, P])} \\ &= \frac{\sum_{x_j \in X} e^{q(x_i)k(x_j)} v(x_j) + \sum_{p_j \in P} e^{q(x_i)k(p_j)} v(p_j)}{\lambda_i(X, [X, P])} \\ &= \frac{\lambda_i(X, X)\mathcal{A}_i(X, X) + \lambda_i(X, P)\mathcal{A}_i(X, P)}{\lambda_i(X, [X, P])} \\ &= f_i(X, P)\mathcal{A}_i(X, X) + h_i(X, P)\mathcal{A}_i(X, P). \end{aligned} \quad (13)$$

Noticing that  $\mathcal{A}(P, [X, P]) = \mathcal{A}(P, [P, X])$ . By following a similar derivation process as Eq. 13, we can deduce the result of prompt forwarding as presented in Eq. 6.

### Additional Implementation Details

Following the previous researches (Zhou et al. 2022b,a; Zhu et al. 2022; Khattak et al. 2023), we implement random resized cropping and flipping into the training process. Additionally, we employ the warm-up technique, whereby the learning rate is initially fixed at  $1e - 5$  for the first epoch before gradually decaying according to the cosine annealing rule from the initial value. In the context of Language-Conditioned Textual Prompting, we have designed specified templates for the text-side input, the majority of which are sourced from CLIP (Radford et al. 2021). These templates are itemized in Tab. 6 for your reference.

### DPL in Extreme Few-shot Scenarios

During our experiment, we made an intriguing observation (e.g., Fig. 5): when confronted with extremely few-shot learning scenarios, vanilla prompt learning methods are prone to overfitting the training set, thereby impairing its performance on the test set. While this issue can be mitigated by employing an additional validation set, it is often challenging to collect sufficient data under this paradigm.

However, we note that our proposed Decoupled Prompt Learning (DPL) effectively curbs the overfitting phenomenon. We hypothesize that this is partially due to our decoupled attention mechanism, which avoids redundant computations and unnecessary interactions. Such reductions can prevent the model from focusing too much on specific input instances from the training set, and instead allow it to prioritize task-specific information. Further investigation into this intriguing phenomenon will be deferred to future research.

<b>Caltech101</b>	a photo of a [CLS], a type of rendition.
<b>OxfordPets</b>	a photo of a [CLS], a type of pet.
<b>StanfordCars</b>	a photo of a [CLS].
<b>Flowers102</b>	a photo of a [CLS], a type of flower.
<b>Food101</b>	a type of food, a photo of [CLS].
<b>FGVCAircraft</b>	a photo of a [CLS], which is a type of an aircraft.
<b>SUN397</b>	a photo of a [CLS].
<b>DTD</b>	a photo of a [CLS], a type of a texture.
<b>EuroSAT</b>	a centered satellite photo of [CLS].
<b>UCF101</b>	a photo of a person doing [CLS].
<b>ImageNet</b>	a photo of a [CLS].
<b>ImageNetV2</b>	a photo of a [CLS].
<b>ImageNet-Sketch</b>	a photo of a [CLS], a type of sketch.
<b>ImageNet-A</b>	a photo of a [CLS], which is natural adversarial.
<b>ImageNet-R</b>	a photo of a [CLS], a type of rendition.

Table 6: **Handcrafted templates used in Language-Conditioned Textual Prompting.**

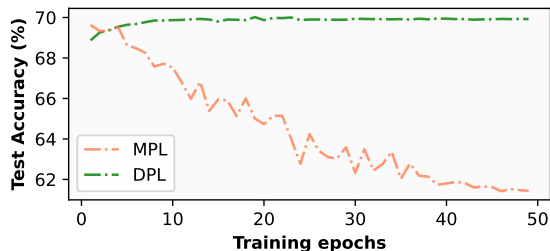


Figure 5: **Record of the training epochs and corresponding testing accuracy on ImageNet in a 1-shot setting.**

### Attention Map Visualization

As we recombine the computation processes of  $\mathcal{A}(X, X)$ , we empirically analyze the impact of the different prompt learning methods on the attention map within instance embeddings. Specifically, we focused on the last transformer layer, which is closest to the final output. To calculate each value of the attention map, we utilized the ‘[CLS]’ token as the query, and all instance embeddings as the key. We then visualize the differences in the attention map between the prompt learning method and the zero-shot CLIP from the visual side, as depicted in Fig. 6. Our results demonstrate that DPL preserves the correlations between input instance embeddings in the last layer much better than vanilla prompt learning. This empirical finding indicates that the original computation structure of the zero-shot CLIP model is well-preserved in earlier layers by DPL, which contributes to our superior generalization performance.

### DPL on Different Backbone Scales

In addition to the ablation studies across different modalities, we have further validated the versatility of our proposed DPL by conducting ablation experiments on two other

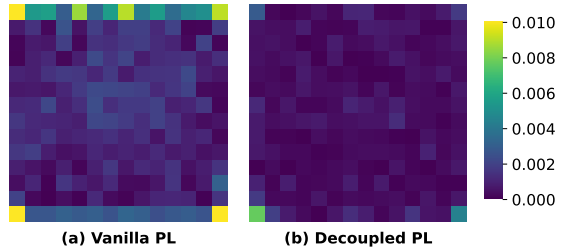


Figure 6: **Visualization of the distance between the attention map generated by two prompt learning methods (vanilla and DPL) and zero-shot CLIP.** Each value of the attention map is calculated using the ‘[CLS]’ token as the query, instance embeddings as the key, and averaging over the entire ImageNet test set.

Methods	Backbone	Base	New	H
CLIP		67.23	71.80	69.44
MPL*	ViT-B/32	79.34	67.60	73.00
DPL		79.78	71.09(+3.49)	75.18
CLIP		69.34	74.22	71.70
MPL*	ViT-B/16	83.57	73.62	78.28
DPL		83.42	75.76(+2.14)	79.40
CLIP		76.65	80.34	78.45
MPL*	ViT-L/14	86.47	77.10	81.52
DPL		86.72	81.21(+4.11)	83.88

Table 7: **Ablation of our proposed DPL on various backbone scales.** We compare DPL with vanilla multi-modal prompt learning (MPL) equipped with LCTP, denoted as MPL\*.

backbone scales: ViT-B/32 based CLIP and ViT-L/14 based CLIP (Radford et al. 2021). In the Base/32 case, we reduce the number of visual prompts per layer to 4 to accommodate the halving of the number of input visual embeddings. For the Large/14 case, we increase the number of visual prompts per layer to 9 and the number of layers for prompt insertion to 18. Additionally, we lower the learning rate of the visual side to 0.02 to stabilize the training process.

As illustrated in Tab. 7, our method yields significant improvements in the accuracy of new categories while maintaining the base performance. Specifically, DPL achieves a 3.49% and 4.11% increase in accuracy on the Base/32 and Large/14 scales, respectively, leading to a substantial improvement in the harmonic mean. These results provide further compelling evidence of the versatility and effectiveness of our approach. Remarkably, as DPL shows a greater improvement of the performance on new classes when the size of the foundational model grows, it indicates that our method holds the potential to be extended to more powerful models, and could enhance the generalization ability in even more challenging tasks.

### Detailed Ablation Results

Due to space limitations in the main paper, we have only presented the average results across 11 datasets in our ablation study. For the convenience of future studies, we include the detailed results in Tab. 8.

Methods	Average			ImageNet			Caltech101			OxfordPets		
	Base	New	H	Base	New	H	Base	New	H	Base	New	H
MaPLe	82.28	75.14	78.55	76.66	70.54	73.47	97.74	94.36	96.02	95.43	97.76	96.58
MaPLe*	82.26	75.30	78.63	76.66	70.51	73.46	97.98	93.71	95.80	95.62	97.86	96.73
MPL	83.48	72.42	77.55	77.29	68.56	72.66	98.21	93.19	95.63	95.21	97.33	96.26
MPL + DA	83.21	74.51	78.62	77.14	70.39	73.61	98.17	94.98	96.55	95.18	97.41	96.28
MPL + DASR	83.15	74.93	78.83	77.24	70.51	73.72	98.15	94.94	96.52	95.52	97.58	96.54
DPL <sub>layers/2</sub>	81.11	75.19	78.04	76.29	70.67	73.37	97.87	94.40	96.10	95.22	97.37	96.28
DPL <sub>tokens/2</sub>	73.65	74.89	74.26	93.37	75.60	83.55	90.73	91.57	91.15	36.77	35.97	36.37
VPL*	80.80	71.23	75.72	75.80	68.41	71.92	98.04	93.23	95.57	95.22	95.55	95.38
VPL* + DASR	80.60	74.03	77.18	75.70	69.42	72.42	98.06	93.67	95.81	95.27	96.65	95.96
TPL*	82.53	72.84	77.38	76.68	68.53	72.38	98.24	94.87	96.53	94.86	97.33	96.08
TPL* + DASR	82.09	74.79	78.27	76.69	71.04	73.76	98.11	94.83	96.44	95.32	97.62	96.46
MPL*	83.57	73.62	78.28	77.05	69.10	72.86	98.54	93.92	96.17	95.71	97.48	96.59
MPL* + DASR	83.42	75.76	79.40	77.17	70.92	73.91	98.08	94.54	96.28	95.34	97.89	96.60
DPL	83.42	75.76	79.40	77.17	70.92	73.91	98.08	94.54	96.28	95.34	97.89	96.60

Methods	StanfordCars			Flowers102			Food101			FGVCAircraft		
	Base	New	H	Base	New	H	Base	New	H	Base	New	H
MaPLe	72.94	74.00	73.47	95.92	72.46	82.56	90.71	92.05	91.38	37.44	35.61	36.50
MaPLe*	72.41	73.90	73.15	96.11	73.19	83.10	90.51	91.97	91.23	37.05	35.81	36.42
MPL	77.50	71.97	74.63	97.53	71.63	82.60	90.05	91.15	90.60	38.12	33.89	35.88
MPL + DA	76.10	74.34	75.21	96.74	73.45	83.50	90.53	91.38	90.95	39.06	34.91	36.87
MPL + DASR	75.96	74.48	75.21	96.55	74.04	83.81	90.53	91.45	90.99	39.36	34.51	36.78
DPL <sub>layers/2</sub>	73.65	74.89	74.26	93.37	75.60	83.55	90.73	91.57	91.15	36.77	35.97	36.37
DPL <sub>tokens/2</sub>	72.14	75.70	73.88	91.82	76.38	83.39	90.74	91.67	91.20	35.43	37.51	36.44
VPL*	71.55	71.82	71.68	91.00	68.89	78.42	90.01	90.70	90.35	34.75	33.07	33.89
VPL* + DASR	71.01	73.20	72.09	90.73	72.72	80.73	90.41	90.71	90.56	34.55	35.51	35.02
TPL*	75.10	72.05	73.54	97.41	73.78	83.96	89.53	91.09	90.30	39.28	34.23	36.58
TPL* + DASR	75.48	75.28	75.38	95.82	76.05	84.80	90.66	91.74	91.20	38.82	36.19	37.46
MPL*	77.05	73.76	75.37	97.34	73.26	83.60	90.37	91.35	90.86	39.70	33.81	36.52
MPL* + DASR	76.16	74.86	75.50	96.39	75.77	84.85	90.46	91.45	90.95	40.40	36.43	38.31
DPL	76.16	74.86	75.50	96.39	75.77	84.85	90.46	91.45	90.95	40.40	36.43	38.31

Methods	SUN397			DTD			EuroSAT			UCF101		
	Base	New	H	Base	New	H	Base	New	H	Base	New	H
MaPLe	80.82	78.70	79.75	80.36	59.18	68.16	94.07	73.23	82.35	83.00	78.66	80.77
MaPLe*	80.47	78.13	79.28	80.29	60.83	69.22	94.11	73.95	82.82	83.68	78.46	80.99
MPL	81.67	77.05	79.29	82.25	50.89	62.88	95.25	65.94	77.93	85.18	74.98	79.76
MPL + DA	80.46	78.89	79.67	81.36	60.87	69.64	95.39	65.57	77.72	85.23	77.41	81.13
MPL + DASR	80.65	79.11	79.87	81.60	61.75	70.30	94.33	68.07	79.08	84.76	77.77	81.11
DPL <sub>layers/2</sub>	79.43	78.68	79.05	78.58	64.41	70.79	86.31	63.79	73.36	83.97	79.74	81.80
DPL <sub>tokens/2</sub>	78.21	78.43	78.32	77.77	65.62	71.18	91.24	69.58	78.95	82.42	80.89	81.65
VPL*	79.81	76.35	78.04	79.98	52.09	63.09	88.36	60.36	71.72	84.30	73.09	78.30
VPL* + DASR	78.03	78.10	78.06	73.54	58.29	65.03	95.74	69.21	80.34	83.52	76.89	80.07
TPL*	81.72	76.53	79.04	80.17	55.84	65.83	90.17	61.92	73.42	84.62	75.10	79.58
TPL* + DASR	80.82	78.66	79.73	79.44	60.51	68.69	88.86	61.56	72.73	83.01	79.16	81.04
MPL*	81.68	77.45	79.51	81.29	56.68	66.79	94.30	64.68	76.73	86.20	78.28	82.05
MPL* + DASR	81.11	78.84	79.96	81.48	63.53	71.39	95.62	69.31	80.37	85.38	79.79	82.49
DPL	81.11	78.84	79.96	81.48	63.53	71.39	95.62	69.31	80.37	85.38	79.79	82.49

Table 8: **Detailed ablation results in base-to-new setting across 11 datasets.** ‘\*’ denotes the model equipped with LCTP, ‘DA’ represents the Decoupled Attention, and ‘DASR’ refers to the Decoupled Attention with Self-attention within prompts Removed.